RSC Advances

PAPER

View Article Online
View Journal | View Issue

Cite this: *RSC Adv.*, 2022, **12**, 31629

Effect of maleic anhydride grafted poly(lactic acid) on rheological behaviors and mechanical performance of poly(lactic acid)/poly(ethylene glycol) (PLA/PEG) blends

Songting Yu,[a] Yiting Zhang,[a] Huan Hu,[a] Juncheng Li,[a] Weiyi Zhou,[ab] Xipo Zhao *[ab] and Shaoxian Peng[ab]

A series of polylactic acid (PLA)/polyethylene glycol (PEG) blends was prepared by melt blending using PEG as a plasticizer to address the disadvantages of PLA brittleness. PEG can weaken the intermolecular chain interactions of PLA and improve its processing properties. PLA-grafted maleic anhydride (GPLA) was reactively blended with PLA/PEG to obtain a high tenacity PLA/PEG/GPLA blend. GPLA was prepared by melt grafting using diisopropyl peroxide as the initiator and maleic anhydride as the graft. The effects of different PEG molecular weights (1000–10 000 g mol^{-1}) on the properties of PLA/PEG/GPLA blends were investigated. GPLA reacted with PEG1000 (M_w = 1000 g mol^{-1}) to form short PLA branched chains and reacted with PEG10000 (M_w = 10 000 g mol^{-1}) to form a small number of PLA branched chains, which was unconducive to increasing the intermolecular chain entanglement. The branched PLA formed by the reaction between PEG6000 (M_w = 6000 g mol^{-1}) and GPLA had a remarkable effect on increasing intermolecular chain entanglement. The complex viscosity, modulus, and melt strength values of PLA/PEG6000/GPLA blends were relatively large. The elongation at break of the blends reached 526.9%, and the tensile strength was 30.91 MPa. It provides an effective way to prepare PLA materials with excellent comprehensive properties.

Received 7th June 2022
Accepted 28th October 2022

DOI: 10.1039/d2ra03513h

rsc.li/rsc-advances

1. Introduction

As a completely degradable polyester polymer material, polylactic acid (PLA) has received increasing attention from scholars due to its good biocompatibility, high modulus, and high strength mechanical properties. With the introduction of PLA, its development has been limited by its inherent disadvantages of low elongation at break, poor impact strength, and brittleness, thereby requiring the toughening modification of PLA.[1–5]

One of the common means of toughening is to blend PLA with thermoplastic elastomer or rubber particles to utilize the inherent high elasticity of the latter and improve the toughness of PLA.[6] However, the addition of rubber will destroy the biodegradability of PLA. PBAT, PBS, PCL, and other elastomers are less compatible with PLA, and achieving the expected toughening effect is difficult. The introduction of some high boiling point, low volatility plasticizers and PLA blending increase the spacing and improve the mobility of the PLA molecular chain.[7] However, PLA plasticizing and toughening is a better method. The addition of plasticizers is often accompanied by a decrease in the glass transition temperature, modulus, and melt viscosity of PLA, thereby promoting the improvement of toughness. This process can also refine the grains and improve the crystallinity of crystalline PLA, so that the tensile and impact toughness of PLA can be improved. PLA plasticizers include small molecular phthalates,[8] citrate esters,[9,10] castor oil,[11] and epoxidized soybean oil.[12,13] Medium molecules include polyethylene glycol (PEG)[14–18] and lactic acid oligomers.[19,20] Buong *et al.*[21] prepared PLA/PEG200 by melt blending using PEG200 (molecular weight 200 g mol^{-1}) as a plasticizer and investigated the mechanical properties and thermal stability of the blends. The introduction of a small amount of PEG200 has no obvious effect on the toughness of PLA. When the content of PEG200 exceeds 10 wt%, the elongation at break of PLA/PEG200 blend reaches 413.1%, and the tensile strength and elastic modulus decrease significantly. Li *et al.*[22–24] systematically studied the effects of PEG on the mechanical, crystallization, and rheological properties of PLA. The results show that in the low content range of PEG, the tensile toughness of PLA increases significantly with the increase in PEG content. In the high content range, the tensile toughness of PLA first decreases and then increases with the increase in PEG content. The change is due to the compatibility

[a]Hubei Provincial Key Ldaboratory of Green Materials for Light Industry, New Materials and Green Manufacturing Talent Introduction and Innovation Demonstration Base, Hubei University of Technology, Wuhan 430068, China. E-mail: xpzhao123@163.com
[b]Hubei Longzhong Laboratory, Xiangyang 441000, China

and crystallization behavior of PLA and PEG. With the increase in PEG molecular weight, the tensile strength and modulus of PLA/PEG blend increase, the elongation at break decreases, and the crystallinity first decreases and then increases due to the dispersion and entanglement of PEG.

PEG acts as a plasticizer, which can easily lead to a significant drop in the blend modulus and melt strength, and plasticizer migration will cause the material to become brittle again. Abstracting tertiary carbon and hydrogen atoms in the long chain of PLA through free radical reaction is assumed to better fix PEG on PLA and reduce its migration. He[43] prepared MPOE by blending MAH and POE through free radical grafting and then added it to PLA to obtain the blend. Compared with PLA/POE blend system, the elongation at break increased from 50.20% to 225.53%. Sommai[44] prepared PP-*g*-MAH by free radical grafting of MAH and PP and added it to PLA/PP blend system as a compatibilizer. They studied the change of phase morphology of PLA/PP/PP-*g*-MAH blend system and found that after adding PP-*g*-MAH, the compatibility was improved, and the blends had an obvious ductile fracture. Much literature had proved that the anhydride group can achieve the purpose of reactive compatibilization in the process of mixing MAH and PLA. We prepared GPLA graft by melt grafting and used it in the PLA/PEG plasticizing system. Maleic anhydride is introduced as a branched chain, and the carboxyl group after the ring opening of maleic anhydride reacts with the terminal hydroxyl group of PEG to form an ester bond, which can better fix PEG between the molecular chains. In this work, PLA-grafted maleic anhydride (GPLA) is prepared by melt grafting and blended with PLA and PEG of different molecular weights to obtain high toughness PLA/PEG/GPLA blends, thereby providing new ideas to improve the migration of plasticizers in PLA plasticizing system.

2. Experimental

2.1 Materials

PLA (4060D) with a glass transition temperature of 55–60 °C was provided by NatureWorks LLC. The used PLA had a density of 1.24 g cm^{-3} and a melt flow index of around 16 g/10 min (210 °C, 2.16 kg). PEG with a weight average molecular weight of 1000–10 000 g mol^{-1} was purchased from Sinopharm Chemical Reagent Co. Ltd (China).

2.2 Sample preparation

2.2.1 Preparation of GPLA. The PLA was dried in a drying oven at 60 °C for 12 h, and the GPLA was prepared by melt blending. A certain amount of PLA and MAH was added to a torque rheometer, the temperature was set to 180 °C, and the speed was 60 rpm. Diisopropyl peroxide was added after mixing for 1.5 min, the mixing was continued for 7.5 min, and the pellet was removed and set aside. For the purification of graft, the method of dissolution followed by precipitation was used.[25–27] The product was taken into a single flask with GPLA using dichloromethane (CH_2Cl) as the solvent, placed in an 85 °C water bath, refluxed until completely dissolved, and precipitated in excess anhydrous ethanol (C_2H_5OH). The dissolution–precipitation operation was repeated three times before the product was dried in a vacuum drying oven.

2.2.2 Preparation of PLA/PEG/GPLA. The PLA, PEG, and GPLA were dried in a vacuum drying oven at 60 °C for 24 h. They were then added to a Harp torque rheometer (RM-200C, Harbin Harper Electric Co.) by one-step mixing for 10 min. The temperature was set to 180 °C, and the rotor speed was set to 60 rpm. The ratio of fixed PLA to PEG were 80/20 and 85/15, and GPLA was added at 5wt% of the total mass. The numbers in PEG1000, PEG4000, PEG6000, PEG8000, and PEG10000 represent the molecular weight of PEG.

2.3 Characterizations

2.3.1 Fourier transform infrared spectroscopy (FT-IR). The purified GPLA was analyzed and tested by FT-IR (Bruker 6700, Bruker, Germany) to determine the reaction between MAH and PLA during the melt blending process. The test sample was obtained by dissolving the fully dried GPLA in CH_2Cl and adding a small amount of the solution dropwise to potassium bromide (KBr) tablets. The mode was set to transmit with a resolution of 4 cm^{-1}, and the scans were from 4000 cm^{-1} to 400 cm^{-1} with 32 times of scanning.

2.3.2 Proton nuclear magnetic resonance (^{1}H-NMR) spectroscopy. ^{1}H-NMR (Ascend 400, Bruker, Germany) was used to determine the structure and molecular characteristics of the PLA and GPLA.

2.3.3 Tensile property testing. An Instron universal testing machine (CMT4000, Meters Industrial Systems Co.) was used to measure the tensile property of the PLA/PEG and PLA/PEG/GPLA blends. Tensile tests were performed at room temperature and a constant cross-head speed of 15 mm min^{-1}. At least five specimens were tested for each reported value. The sample was made into 10 cm × 10 cm × 2 mm plate with a flat vulcanizing machine (XLB-300X3, China Qingdao Jinjiuzhou Rubber Machinery Co.) and then cut into 10 cm × 1.5 cm × 2 mm long strip. The test sample was made by using the mold of universal sample making machine (XYZ, Chengde Jinjian Testing Instruments Co.) with reference to the ISO 527-2 standard.

2.3.4 Impact property testing. An impact test machine was used to test the notched impact performance of PLA/PEG and PLA/PEG/GPLA blends. The impact energy was set to 0.5 J, and the test results were the average of at least 5 valid sample data. The sample was made into 10 cm × 10 cm × 4 mm plate by flat vulcanizing machine and then cut into 10 cm × 1.5 cm × 4 mm long strip. The test strips were prepared by using a notched sample preparation machine (JJANM-11, Chengde Jinjian Testing Instruments Co.) with reference to the ISO 179-1 standard.

2.3.5 Dynamic mechanical analysis. The dynamic mechanical properties of the samples were measured by using a dynamic mechanical spectrometer (Q800, TA Instruments, Inc.) with a tensile mode at a frequency of 1 Hz. The scanning temperature was from −80 °C to 100 °C at a heating rate of 3 °C min^{-1}, and nitrogen gas protection was needed in the whole process. The dimensions of the samples were 12.5 mm × 17.5 mm × 2 mm.

2.3.6 Rheological measurements. Rotational rheometers (DHR-2, TA Instruments, Inc.) were used to test the viscosity and modulus of the blends. The test mode was the frequency scan mode, the strain was set to 0.1%, and the scan range was 0.1 Hz to 100 Hz at the experimental temperature of 170 °C. Capillary rheometers (Rheograph 25, Göttfert, Germany) were used to test the tensile rheological behavior of the blends. The extrusion temperature was set to 170 °C, the extrusion rate was 0.5 mm s^{-1}, and the initial melt stretching rate was 40 mm s^{-1}.

3. Results and discussion

3.1 FTIR

The characteristic absorption peak of the C=O double bond in MAH appeared near 1780 cm^{-1}, showing a strong symmetric stretching vibration, and the asymmetric stretching vibration peak showed a weak signal peak near 1845 cm^{-1}.[28,29] Fig. 1 shows the FT-IR curves of PLA and GPLA. The characteristic absorption peak of C=O in PLA was similar to that of MAH, and the peak positions of the two peaks overlapped, so that the strong characteristic peak of MAH near 1780 cm^{-1} was obscured. Grafting was usually determined by the weak peak of MAH near 1845 cm^{-1},[30,31] and GPLA showed a weak peak near 1845 cm^{-1}, indicating the grafting reaction of MAH with PLA.

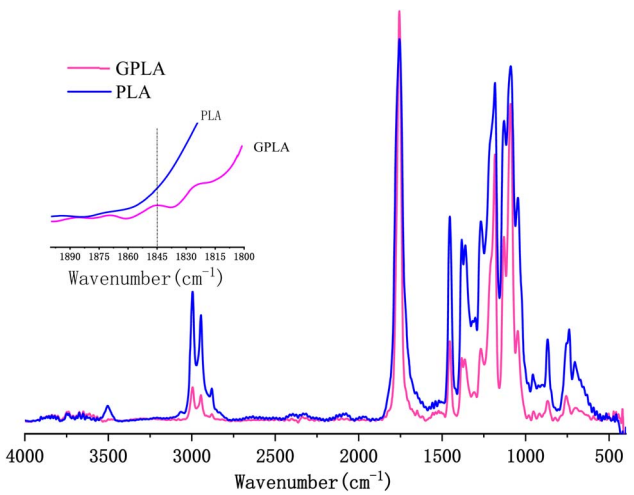

Fig. 1 .FT-IR spectra of the PLA and GPLA.

Through DCP initiation, hydrogen on the tertiary carbon of PLA molecular chain was captured to form tertiary carbon free radical, which was connected with the double bond on MAH, so as to realize grafting (Fig. 2).

3.2 ^{1}H-NMR spectroscopy

The ^{1}H-NMR testing analyzed the structure of GPLA. Fig. 3 shows the ^{1}H-NMR results of PLA and GPLA, and four distinct peaks in the range of 0 ppm to 10 ppm appear for pure PLA. Among them, the signal at 7.2 ppm represents the peak of the deuterated chloroform solution, and the peaks near 1.6 and 5.2 ppm represent the hydrogen on the PLA methylene and hypomethyl groups, respectively. New peaks appeared in the spectrum of GPLA, with more distinct peaks at 3.8 and 1.3 ppm. The signal peak at 3.8 ppm was attributed to the hydrogen in MAH methylene, and the signal peak at 1.3 ppm was due to the chemical shift of the free radical to the PLA backbone after the β-break. The intensity of PLA signal peaks near 1.6 and 5.2 ppm decreased, especially the peak position of the tertiary hydrocarbon representative at 5.2 ppm decreased significantly, indicating that MAH grafted at the position of PLA tertiary carbon to form GPLA.

3.3 Effects of different PEG molecular eights on the mechanical properties of PLA/PEG/GPLA

A relatively positive plasticizing effect was observed when the content of PEG in the blend was 20 wt%,[40] and the PEG was partially agglomerated and showed obvious phase separation[41] without plasticizing effect when the content was higher than 20 wt%. Fig. 4 shows the effects of different PEG molecular weights on the mechanical properties of PLA/PEG (80/20) and PLA/PEG/GPLA (80/20/5) blends. It can be seen from Fig. 5) that the blends prepared in this work have excellent comprehensive mechanical properties compared with PLA/PEG blends reported in some literatures.[32–39] The tensile toughness of PLA/PEG blends with PEG content at 20 wt% was lower than that of PLA/PEG/GPLA. This finding was due to the reaction of GPLA with PEG to form branched PLA for promoting the dispersion of PEG and toughening PLA. The blend plasticized by PEG6000 had better tensile toughness, indicating that PEG6000 was favorable to increase the free volume of PLA and to react with GPLA to form branched PLA (Fig. 6). The branched PLA

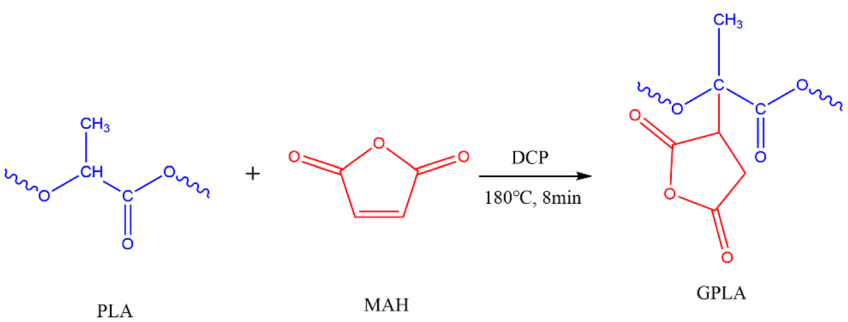

Fig. 2 .Reaction formula of grafting MAH onto PLA.

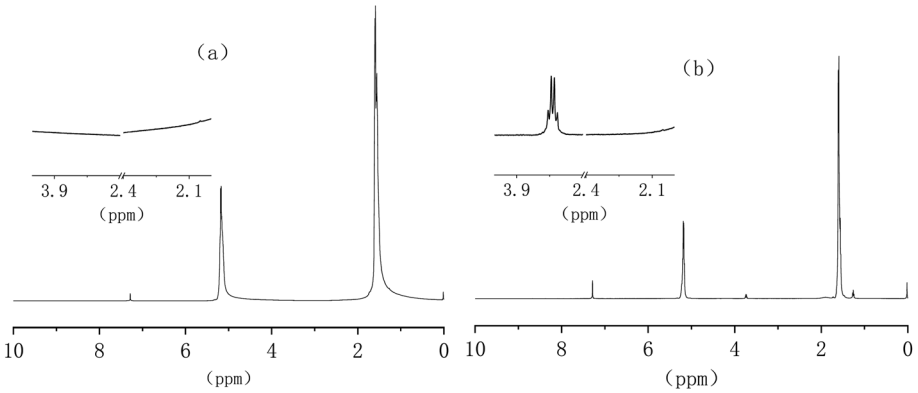

Fig. 3 .[1]H-NMR spectrum of the grafts of PLA (a) and GPLA (b).

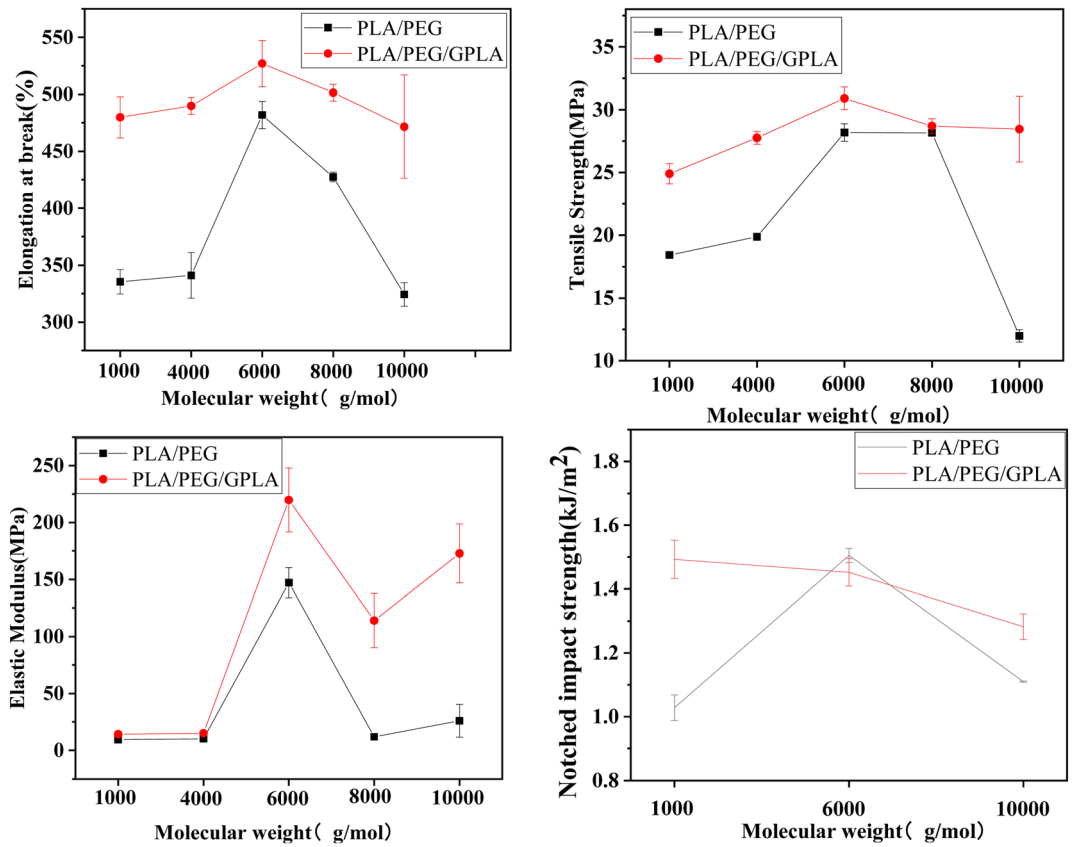

Fig. 4 .Effects of different PEG molecular weights on the tensile and impact toughness of PLA/PEG(80/20) and PLA/PEG/GPLA(80/20/5).

increased to form more physical entanglement with the PLA matrix, which was favorable to the improvement of toughness. The elongation at break of the PEG1000 plasticized blends increased significantly after the addition of GPLA. This finding was due to the weak plasticizing effect caused by the agglomeration of excess PEG1000. The addition of GPLA promoted the dispersion of PEG1000, and the formation of short-branched PLA increased the interaction with the substrate. PEG10000 had larger molecular weight and less terminal groups, and the elongation at break of the blends became unstable after the addition of GPLA although they increased. In terms of impact toughness, PEG6000 formed good dispersion in the PLA matrix, so the impact strength of the blends did not change significantly with or without the addition of GPLA. PEG1000 and PEG10000 depended on GPLA to form better dispersion and good interaction with the matrix, thereby improving the toughness of the blends.

The branching compound formed by the reaction of PEG with GPLA with lower molecular weight was conducive to the plasticization of PLA, and the lack of reactive groups with higher

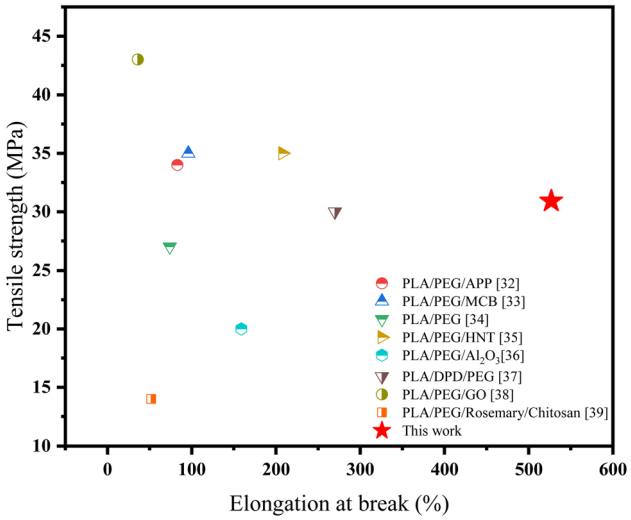

Fig. 5 .Comparison of the tensile strength and elongation at break between PLA/PEG6000/GPLA(80/20/5) and PLA/PEG blends reported in some literatures.[32–39]

molecular weight makes it difficult to form branching compounds, resulting in a downward trend in the plasticization effect. The branched PLA formed by the reaction of PEG6000 and GPLA in the blend had moderate branched chain length and branched chain density, which was conducive to the formation of entanglement with PLA molecular chains. The entanglement of GPLA and PLA molecular chains is conducive to improving the viscosity, modulus and melt strength of PLA/PEG/GPLA blends, and even further increasing the mechanical properties of the blends. At the same time, according to the theory of similar solubility, the PEG branched chains on branched PLA were easy to interact with free PEG, this entanglement network may limit the migration of PEG molecules and increase the stability of the blends.

3.4 Effects of different PEG molecular weights on the dynamic mechanical properties of PLA/PEG/GPLA

In the PLA/PEG/GPLA system with high content of PEG, the reaction of GPLA and PEG to form branched PLA further improved the tensile toughness of the blends. T_g is affected by branched PLA together with PEG. Fig. 7 shows the dynamic mechanical property curves of the blends prepared with different molecular weights of PEG. From the storage modulus–temperature curve, the storage modulus of PLA experienced three steps: a gentle decrease – a rapid decrease – a gentle decrease with the increase in temperature, indicating that PLA relaxed only once in this temperature range. The PLA/PEG1000/GPLA blend had a higher storage modulus than PLA at a lower temperature. This finding was because the temperature has exceeded the glass transition temperature of PEG, and the plasticizing effect of PEG1000 was remarkable. With the increase in temperature, the mobility of PLA molecular chains increased, and the internal stress and storage modulus decreased rapidly. With the increase in the molecular weight of PEG, the slope of the storage modulus gradually decreased in the rapid decline stage, indicating that in addition to the plasticizing effect of PEG, the physical entanglement increased in the blend, and higher PEG molecular weight led to slower relaxation. The relaxation speed of the sample can be judged in

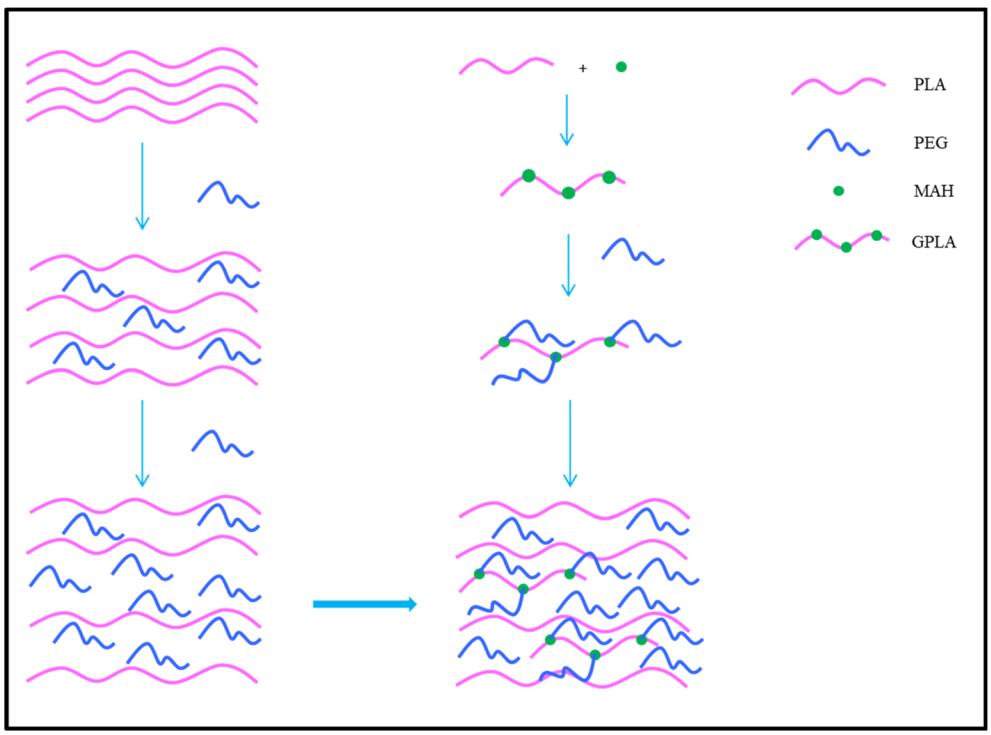

Fig. 6 .The schematic diagram of PEG acting on PLA and reacting with GPLA to form branched PLA.

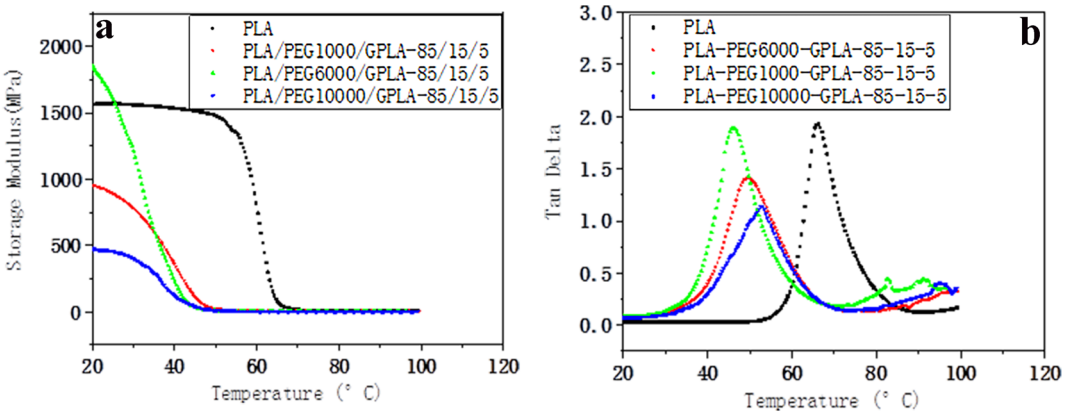

Fig. 7 . Variation curve of the storage modulus (a) and loss factor (b) of blends prepared with different PEG molecular weights with temperature.

accordance with the peak value of the loss factor. From the loss factor–temperature curve, PLA has the largest peak value of the loss factor. T_g was 69 °C, and the peak loss factor decreased after the addition of PEG, indicating that the internal stress of the blends decreased after PLA was plasticized by PEG. With the increase in the molecular weight of PEG, the peak value of the loss factor of the blends decreased, and the corresponding T_g increased. The T_g values of PLA/PEG1000/GPLA blend, PLA/PEG6000/GPLA blend, and PLA/PEG10000/GPLA blend were 47 °C, 50 °C, and 52 °C, respectively, due to the higher plasticizing effect. Higher molecular weight PEG formed more physical entanglement with the PLA matrix after reacting with GPLA.

3.5 Effects of different PEG molecular weights on the rheological behavior of PLA/PEG/GPLA

The rheological curves of PLA/PEG/GPLA (80/20/5) blends prepared with different molecular weights of PEG are shown in Fig. 8. From Fig. 8(a), PLA had the largest complex viscosity ($|\eta^*|$), and the PLA/PEG (80/20) blend $|\eta^*|$ decreased significantly after adding 20 wt% PEG. The $|\eta^*|$ value of the PLA/PEG/GPLA (80/20/5) blend increased after the continued introduction of GPLA. This finding was because the reaction of GPLA with PEG to form branched PLA increased the degree of entanglement between the blend components. The ranking of the intercomponent entanglement of the blends was PLA/PEG6000/GPLA > PLA/PEG10000/GPLA > PLA/PEG1000/GPLA, which was obtained from the analysis of the shear thinning behavior in the high-frequency region. This finding was probably due to the shorter branched PLA chains formed by the reaction between GPLA and PEG1000 and the higher density of the branched chains, resulting in a lower degree of intermolecular chain entanglement in the system due to the spatial site resistance effect. The reaction of GPLA with PEG10000 to form longer branched chains of branched PLA tended to cause self-entanglement with limited enhancement of the interaction between PLA and PEG components. However, the formation of entanglement sites with PLA was more likely due to the larger molecular weight of PEG10000. Thus, the $|\eta^*|$ value of PLA/PEG10000/GPLA (80/20/5) was slightly higher than that of PLA/PEG1000/GPLA (80/20/5). PEG6000 had the suitable molecular chain length and number of reactive sites for the same mass, so the PLA/PEG6000/GPLA blend had the maximum $|\eta^*|$ value.

Fig. 8(b) and (c) show the storage modulus (G') and loss modulus (G'') of the PLA/PEG/GPLA (80/20/5) blends, with approximately the same trend as the viscosity. PEG as a plasticizer weakened the intermolecular entanglement of PLA chains, resulting in a decrease in the G' and G'' curves of PLA/PEG6000 blends. The reaction of GPLA with PEG to form branched PLA increased the adhesion between the components of the blends, and the G' and G'' curves of the PLA/PEG/GPLA (80/20/5) blends increased significantly after the introduction of GPLA. The slopes at the end of the Han curves of PLA/PEG1000/GPLA, PLA/PEG6000/GPLA, and PLA/PEG10000/GPLA blends in Fig. 8(d) were similar, indicating that the effect of PEG molecular weight size on the compatibility of PLA was weak. The reaction of PEG6000 in the system to form branched PLA had a significant effect on the viscoelasticity of the PLA/PEG/GPLA system, which was judged by the magnitude of the end of the curve.

Fig. 8(e) shows the variation curves of G' and G'' with frequency for different PEG molecular weights. The G' and G'' curves of PLA had a crossover point in the frequency range, whereas the PLA/PEG6000 (80/20) blend had no crossover point in the frequency range, indicating that the PEG plasticization was beneficial to increase the elasticity of the blend but weakened the intermolecular chain entanglement effect of the blend. The PLA/PEG1000/GPLA blend had no intersection in the frequency range, and the degree of opening at the high frequency end was larger. The PLA branched chain length formed by the reaction between GPLA and PEG1000 was probably extremely short, and the branched chains were extremely dense, resulting in obvious site-blocking effect, and the branched PLA showed more plasticizing effect in the blended system at this time. The G' and G'' curves of PLA/PEG6000/GPLA blends showed an insignificant crossover point at the end of high frequency, indicating that PEG molecular weight had a significant effect on the viscoelastic transition of PLA/PEG/

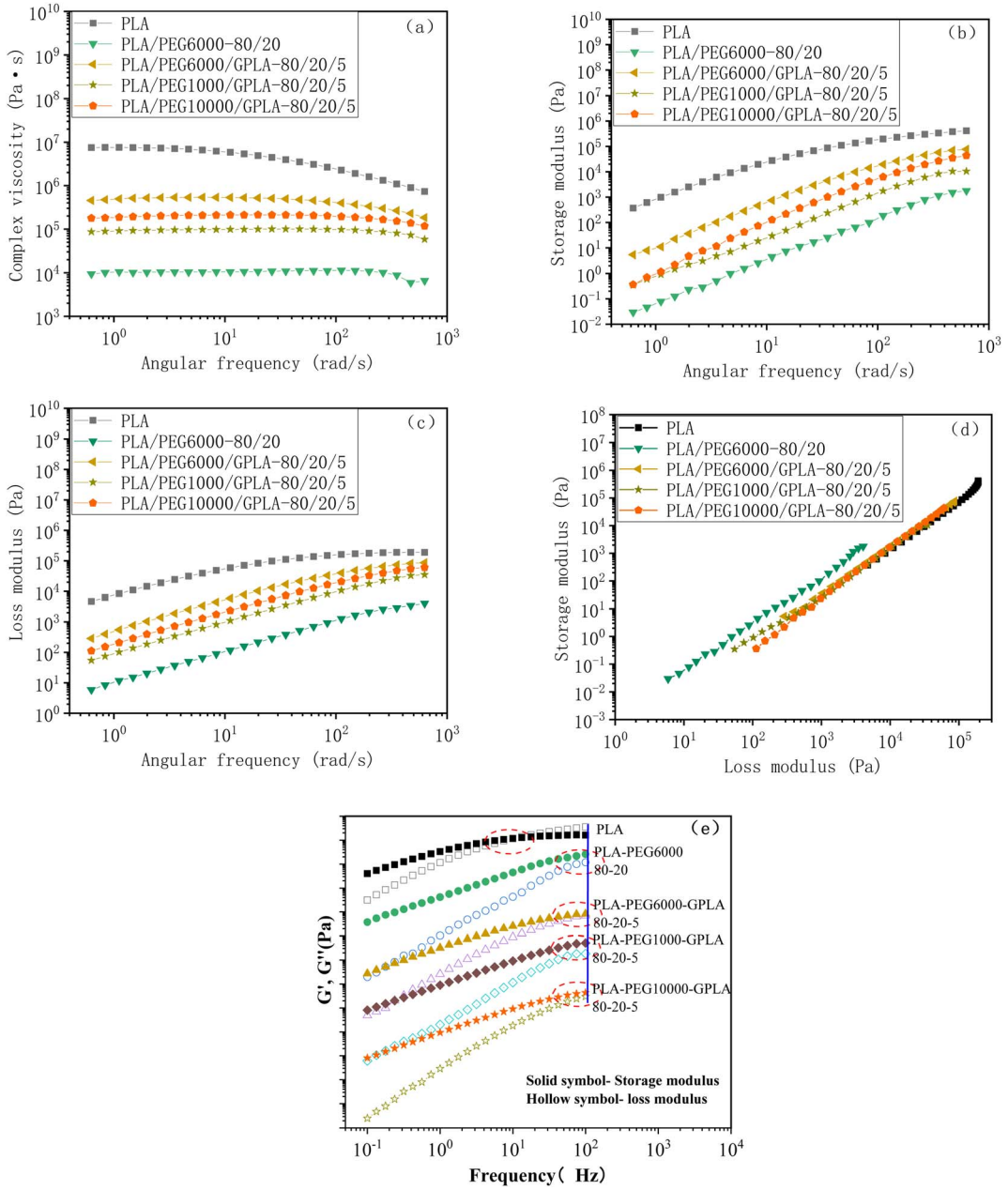

Fig. 8 .Rheological curves of PLA, PLA/PEG6000, PLA/PEG1000/GPLA, PLA/PEG6000/GPLA, and PLA/PEG10000/GPLA blends: (a) complex viscosity ($|\eta^*|$); (b) energy storage modulus (G'); (c) loss modulus (G''); (d) Han curve; (e) G' and G'' changing curve with frequency.

GPLA blends. When the molecular weight of PEG increased to 10 000, the G' and G'' curves of PLA/PEG10000/GPLA blends had no intersection in the frequency range. This finding might be because the branched chains of the branched PLA formed by the reaction in the system were extremely long, and the long chains were prone to self-entanglement, thereby weakening the entanglement with the chains of PLA molecules. In summary, the molecular weight of PEG directly affected the branched chain length and branched chain density of the branched PLA formed in the system, and the structure of the branched PLA had a significant effect on the viscoelastic transition of the PLA/PEG/GPLA system.

In the PLA/PEG system, the plasticization of PLA by PEG was performed through hydrogen bonding,[42] which transformed the PLA–PLA macromolecular forces into PLA–PEG small molecule interactions. However, physical entanglement was observed between the high molecular weight PEG and PLA molecular chains in addition to hydrogen bonding forces, and this entanglement toughened the PLA together with the plasticizing effect of PEG. The melt strength of the blends with 1000, 6000, and 10 000 g mol^{-1} PEG molecular weight is shown in Fig. 9 as a function of traction rate. The melt strength of PLA/PEG1000/GPLA blend was the lowest at the same rate, indicating that the reaction forming branched PLA with shorter branched

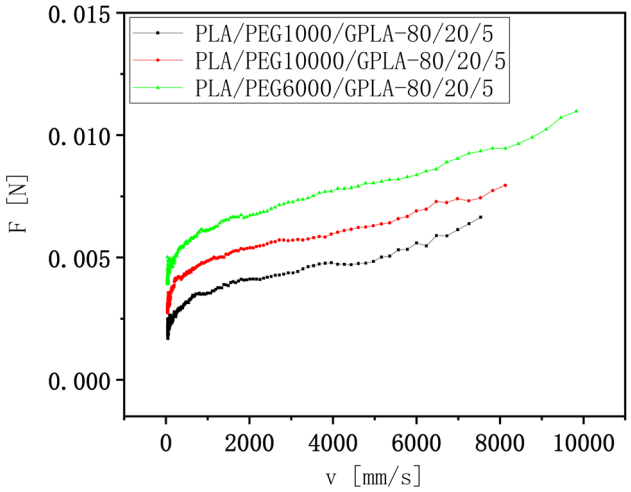

Fig. 9 .Melt strength curve of PLA/PEG/GPLA (80/20/5) blends.

chains was more favorable to produce large free volume rather than increasing physical entanglement. Such short branched chains were more favorable to enhance the mobility of PLA molecular chains with other tail of the curve. The PLA/PEG6000/GPLA blend exhibited greater melt strength, which might be because PEG6000 exceeded the minimum entanglement length for entanglement with PLA, and the branched chains formed by GPLA and PEG formed entanglement with the matrix well, thereby enhancing the melt strength.

4. Conclusion

PLA/PEG blends are prepared by melt blending to improve the brittleness of PLA. The tensile properties of the blends prepared by PEG with molecular weights of 1000, 4000, 6000, 8000, and 10 000 g mol^{-1} are compared, and the PEG with molecular weight of 6000 g mol^{-1} has the best plasticizing effect on PLA. The PLA is melt grafted by using MAH, and a PLA/PEG/GPLA blend with high toughness is prepared to further improve the toughness of the blends. The ring opening of the anhydride group in GPLA reacts with the end groups of PEG to form branched chains, which can better fix PEG in the blends. The branched structure formed increases the free volume between the molecular chains and promotes physical entanglement, thereby improving the toughness of the blends. The elongation at break of the PLA/PEG6000/GPLA (80/20/5) blend can reach 526.9%, with a tensile strength of 30.91 MPa and an elastic modulus of 219.7 MPa. The branched PLA formed by the reaction between GPLA and PEG helps to increase the degree of entanglement between the blend components, avoiding a significant decrease in viscosity, modulus, and melt strength of the blend. This entanglement network also delays the migration of plasticizers, thereby expanding the application of PLA in the packaging and pharmaceutical industries.

Conflicts of interest

There are no conflicts to declare.

Acknowledgements

The work is funded by National Natural Science Foundation of China (51273060; 52073083), and Hubei University of Technology Green Industry Technology Leading Project.

References

1 H. Liu and J. Zhang, Research progress in toughening modification of poly (lactic acid), *J. Polym. Sci., Part B: Polym. Phys.*, 2011, **49**(15), 1051–1083.
2 Y. Yang, L. Zhang, Z. Xiong, *et al.*, Research progress in the heat resistance, toughening and filling modification of PLA, *Sci. China: Chem.*, 2016, **59**(11), 1355–1368.
3 X. Zhao, D. Zhang, S. Yu, *et al.*, Recent advances in compatibility and toughness of poly (lactic acid)/poly (butylene succinate) blends, *e-Polym.*, 2021, **21**(1), 793–810.
4 G. Kfoury, J. M. Raquez, F. Hassouna, *et al.*, Recent advances in high performance poly (lactide): from "green" plasticization to supertough materials *via* (reactive) compounding, *Front. Chem.*, 2013, **1**(32), 2013.
5 J. Jayaramudu, K. Das, M. Sonakshi, *et al.*, Structure and properties of highly toughened biodegradable polylactide/ZnObiocomposite films, *Int. J. Biol. Macromol.*, 2014, **64**, 428–434.
6 L. Zhang, Z. Jiang and Z. Wang, Morphology evolution, mechanical properties, Mullins effect, and its reversibility of polylactide/nitrile butadiene rubber thermoplastic vulcanizates plasticized by dioctyl phthalate, *J. Thermoplast. Compos. Mater.*, 2021, **34**(1), 24–39.
7 Z. Lin, X. Guo, Z. He, *et al.*, Thermal degradation kinetics study of molten polylactide based on Raman spectroscopy, *Polym. Eng. Sci.*, 2020, 1–10.
8 N. Thummarungsan, D. Pattavarakorn and A. Sirivat, Tuning rigidity and negative electrostriction of multi-walled carbon nanotube filled poly (lactic acid), *Polymer*, 2020, **196**, 122488.
9 A. M. El- Hadi, Increase the elongation at break of poly (lactic acid) composites for use in food packaging films, *Sci. Rep.*, 2017, **7**(46767), 1–14.
10 R. Petrucci, E. Fortunati, D. Puglia, *et al.*, Life cycle analysis of extruded films based on poly(lactic acid)/cellulose nanocrystal/limonene: a comparative study with ATBC plasticized PLA/OMMT systems, *J. Polym. Environ.*, 2018, **26**(5), 1891–1902.
11 W. He, H. Huang, L. Xie, *et al.*, The influence of self-crosslinked epoxidized castor oil on the properties of Poly (lactic acid) *via* dynamic vulcanization: Toughening effect, thermal properties and structures, *Colloids Surf., A*, 2021, **630**, 127517.
12 W. Q. Yuan, H. Zhang, Y. X. Weng, *et al.*, Fully biobased polylactide/epoxidized soybean oil resin blends with balanced stiffness and toughness by dynamic vulcanization, *Polym. Test.*, 2019, **78**, 105981.
13 C. Buong, I. Nor, T. Yoon, *et al.*, Epoxidized vegetable oils plasticized poly (lactic acid) biocomposites : mechanical, thermal and morphology properties, *Molecules*, 2014, **19**(10), 16024–16038.

14 B. W. Chieng, N. A. Ibrahim, W. M. Z. Wan Yunus, *et al.*, Poly (lactic acid)/poly (ethylene glycol) polymer nanocomposites: Effects of graphene nanoplatelets, *Polymers*, 2013, **6**(1), 93–104.

15 X. Gao, S. Qi, D. Zhang, *et al.*, The role of poly (ethylene glycol) on crystallization, interlayer bond and mechanical performance of polylactide parts fabricated by fused filament fabrication, *Addit. Manuf.*, 2020, **35**, 101414.

16 N. Sundar, S. J. Stanley, S. A. Kumar, *et al.*, Development of dual purpose, industrially important PLA–PEG based coated abrasives and packaging materials, *J. Appl. Polym. Sci.*, 2021, **138**(21), 50495.

17 H. Hu, A. Xu, D. Zhang, *et al.*, High-toughness poly (lactic acid)/starch blends prepared through Reactive Blending Plasticization and Compatibilization, *Molecules*, 2020, **25**(24), 5951.

18 S. Wasti, E. Triggs, R. Farag, *et al.*, Influence of plasticizers on thermal and mechanical properties of biocomposite filaments made from lignin and polylactic acid for 3D printing, *Composites, Part B*, 2021, **205**, 108483.

19 S. M. Moghaddam, B. Quelennec, N. Delpouve, *et al.*, Fragility of short-chain poly (lactic acid) s derivatives by combining dielectric spectroscopy and fast scanning calorimetry, *J. Polym. Sci.*, 2021, **59**(14), 1571–1577.

20 M. P. Arrieta, M. Perdiguero, S. Fiori, *et al.*, Biodegradable electrospun PLA-PHB fibers plasticized with oligomeric lactic acid, *Polym. Degrad. Stab.*, 2020, **179**, 109226.

21 B. W. Chieng, N. A. Ibrahim, W. M. Z. Wan Yunus, *et al.*, Plasticized poly (lactic acid) with low molecular weight poly (ethylene glycol): Mechanical, thermal, and morphology properties, *J. Appl. Polym. Sci.*, 2013, **130**(6), 4576–4580.

22 F. J. Li, J. Z. Liang, S. D. Zhang, *et al.*, Tensile properties of polylactide/poly (ethylene glycol) blends, *J. Polym. Environ.*, 2015, **23**(3), 407–415.

23 F. J. Li, S. D. Zhang, J. Z. Liang, *et al.*, Effect of polyethylene glycol on the crystallization and impact properties of polylactide-based blends, *Polym. Adv. Technol.*, 2015, **26**(5), 465–475.

24 F. J. Li, L. C. Tan, S. D. Zhang, *et al.*, Compatibility, steady and dynamic rheological behaviors of polylactide/poly (ethylene glycol) blends, *J. Appl. Polym. Sci.*, 2015, **133**(4), 42919.

25 W. Liu, T. Liu, T. Liu, *et al.*, Improving grafting efficiency of dicarboxylic anhydride monomer on polylactic acid by manipulating monomer structure and using comonomer and reducing agent, *Ind. Eng. Chem. Res.*, 2017, **56**(14), 3920–3927.

26 F. Y. Wang, L. Dai, T. T. Ge, *et al.*, α- methylstyrene -assisted maleic anhydride grafted poly(lactic acid) as an effective compatibilizer affecting properties of microcrystalline cellulose/poly (lactic acid) composites, *eXPRESS Polym. Lett.*, 2020, **14**(6), 530–541.

27 G. F. Brito, J. Xin, P. Zhang, *et al.*, Enhanced melt free radical grafting efficiency of polyethylene using a novel redox initiation method, *RSC Adv.*, 2014, **4**(50), 26425–26433.

28 F. Y. Wang, L. Dai, T. T. Ge, *et al.*, α- methylstyrene -assisted maleic anhydride grafted poly (lactic acid) as an effective compatibilizer affecting properties of microcrystalline cellulose/poly (lactic acid) composites, *eXPRESS Polym. Lett.*, 2020, **14**(6), 530–541.

29 G. F. Brito, J. Xin, P. Zhang, *et al.*, Enhanced melt free radical grafting efficiency of polyethylene using a novel redox initiation method, *RSC Adv.*, 2014, **4**(50), 26425–26433.

30 J. Petru, F. Kuera and J. Petrj, Post-polymerization modification of poly (lactic acid) *via* radical grafting with itaconic anhydride, *Eur. Polym. J.*, 2016, **77**, 16–30.

31 I. Domenichelli, S. Coiai, F. Cicogna, *et al.*, Towards a better control of the radical functionalization of poly(lacticacid), *Polym. Int.*, 2015, **64**(5), 631–640.

32 Y. P. Song, D. Y. Wang, X. L. Wang, *et al.*, A method for simultaneously improving the flame retardancy and toughness of PLA, *Polym. Adv. Technol.*, 2011, **22**(12), 2295–2301.

33 Z. Su, K. Huang and M. Lin, Thermal and mechanical properties of poly (lactic acid)/modified carbon black composite, *J. Macromol. Sci. Phys.*, 2012, **51**(8), 1475–1484.

34 B. Wang, K. Hina, H. Zou, *et al.*, Thermal, crystallization, mechanical and decomposition properties of poly (lactic acid) plasticized with poly (ethylene glycol), *J. Vinyl Addit. Technol.*, 2018, **24**, E154–E163.

35 Z. Lule, H. Ju and J. Kim, Thermomechanical properties of alumina-filled plasticized polylactic acid: Effect of alumina loading percentage, *Ceram. Int.*, 2018, **44**(18), 22767–22776.

36 S. Sharma, A. A. Singh, A. Majumdar, *et al.*, Tailoring the mechanical and thermal properties of polylactic acid-based bionanocomposite films using halloysite nanotubes and polyethylene glycol by solvent casting process, *J. Vinyl Addit. Technol.*, 2019, **54**(12), 8971–8983.

37 Y. Jiang, C. Yan, K. Wang, *et al.*, Super-toughed PLA blown film with enhanced gas barrier property available for packaging and agricultural applications, *Materials*, 2019, **12**(10), 1663.

38 J. Ahmed, M. Z. Mulla, A. Vahora, *et al.*, Morphological, barrier and thermo-mechanical properties of high-pressure treated polylactide graphene oxide reinforced composite films, *Food Packag. Shelf Life*, 2021, **29**, 100702.

39 C. Vasile, E. Stoleru, R. N. Darie-Niţa, *et al.*, Biocompatible materials based on plasticized poly (lactic acid), chitosan and rosemary ethanolic extract I. effect of chitosan on the properties of plasticized poly (lactic acid) materials, *Polymers*, 2019, **11**(6), 941.

40 F. Hassouna, J. M. Raquez, F. Addiego, *et al.*, New approach on the development of plasticized polylactide (PLA): Grafting of poly (ethylene glycol)(PEG) *via* reactive extrusion, *Eur. Polym. J.*, 2011, **47**(11), 2134–2144.

41 B. Wang, K. Hina, H. Zou, *et al.*, Thermal, crystallization, mechanical and decomposition properties of poly (lactic acid) plasticized with poly (ethylene glycol), *J. Vinyl Addit. Technol.*, 2018, **24**, E154–E163.

42 Z. Guo, S. Zhang, Y. Liang, *et al.*, Toughness Enhancement of Poly (lactic acid), Bamboo Particle and Ultrafine Bamboo-

Char Ternary Biocomposites by Polyethylene Glycol Plasticization, *J. Polym. Environ.*, 2022, **30**(3), 1162–1169.

43 W. He, L. Ye, P. Coates, *et al.*, Reactive processing of poly (lactic acid)/poly (ethylene octene) blend film with tailored interfacial intermolecular entanglement and toughening mechanism, *J. Mater. Sci. Technol.*, 2022, **98**, 186–196.

44 S. Pivsa-Art, J. Kord-Sa-Ard, W. Pivsa-Art, *et al.*, Effect of compatibilizer on PLA/PP blend for injection molding, *Energy Procedia*, 2016, **89**, 353–360.